Introduction to Experimental Aeroacoustics

Marc C. JACOB
Département d'Aérodynamique Energétique & Propulsion,
ISAE-SUPAERO
10 av. Edouard Belin, B.P. 54032, Toulouse Cedex 4
FRANCE

marc.jacob@isae-supaero.fr

Special thanks. This document has been prepared with inputs from contributors Michel Roger, Bertrand Mercier, Emmanuel Jondeau, Paul Laffay, Stéphane Moreau and Christophe Schram.

ABSTRACT

This introductory lecture gives an overview of the challenges and pitfalls of wind tunnel experiments in aeroacoustics. Most concepts introduced here will be developed in following lectures.

1.0 EXPERIMENTAL AEROACOUSTICS: WHAT FOR?

1.1 The Origin of Experimental Aeroacoustics

Strouhal [1] was probably the first to relate sound generation to fluid motion in 1878 in his experimental investigation of Aeolian tones generated by a stretched wire, but he incriminated fluid friction as the origin of the radiated sound. It was only in 1915 that Lord Rayleigh [2] related the sound radiation to the periodic vortex shedding after discovering that even rigid cylinders produce Aeolian tones when placed in a flow, which really was the beginning of aeroacoustics as a branch of flow physics.

The next jump of aeroacoustics also came along with experimental evidence of the extreme acoustic nuisance caused by the first jet engines that led to the pioneering work of Sir J. Lighthill [4], [5] about the physics of jet noise, followed by many others who investigated the role of solid surfaces in turbulent flows. This advance also revealed a need for aeroacoustic investigations in wind-tunnel experiments, which provided information that could not be measured on real flying aircrafts.

The latest step of aeroacoustics came along with the progress of unsteady high-order Computational Fluid Dynamics (CFD) and CFD in general, that became applicable to aeroacoustic problems [6], [7], [8], [9] giving birth to a new branch of aeroacoustics, Computational AeroAcoustics (CAA). This progress also fostered a new type of aeroacoustic experiments, so-called *benchmark experiments*, whose role it is to provide verification, validation and calibration data for CFD codes.

Today a new age is dawning with the upcoming of highly efficient and versatile CFD methods (such as LBM) on one hand and the rise of high-resolution experimental tools on the other hand. These tools (such as time resolved PIV or multi-sensor pressure arrays based on MEMS technologies) become increasingly accurate, reliable and applicable to aeroacoustic investigations. These developments will certainly deeply modify our approach to aeroacoustics in the next decade: the process has already begun.

1.2 Motivation for Experimental Aeroacoustics

This brief introductory history of aeroacoustics highlights the three types of experimental approaches that are still encountered in our community's wind tunnels as well as the purposes they are designed for.

1.2.1 Fundamental Aeroacoustics

Experiments for fundamental studies in aeroacoustics are meant to characterise basic mechanisms of sound

generation by unsteady flows: they are designed to give clues for and to help both understanding and modelling such mechanisms. Therefore, they are based on simple or simplified configurations in order to rule out spurious mechanisms or installation effects and to isolate the very mechanism that is investigated. Moreover, they are in general suited for parametric studies to test the trend and limits of the underlying mechanism (e.g. the recent study of multiple jets spreading from a perforated plate see Fig 3-1 and 3-6 [13]).

1.2.2 Benchmark Experiments

CAA codes and mixed CFD/CAA approaches require several levels of validation, first against analytical solutions of model problems, secondly against experimental data for slightly more complex configurations. Designing experiments for such purpose requires special care, taking also into account the constraints and weaknesses of CFD (e.g. [15]).

1.2.3 Wind Tunnel Tests Mimicking Real Situations

In many practical applications, aeroacoustics involves vehicles or parts of vehicles (aircrafts, trains, cars, landing gears, exhaust jets of turboengines…) moving in open space: in order to characterise the sound generation by such complex systems, special wind tunnel experiments are designed. Despite the fact that they often take place in large facilities, the tested elements are in general downscaled mock-ups, the ambient airflows are generally limited to a relatively small surrounding region and the experimental set-up is carried out in the vehicle frame of reference. There are many issues to be addressed in order to obtain test conditions that are representative of or can at least be extrapolated to the real situation. In particular, boundaries are extremely important in aeroacoustics.

The situation is less ambiguous if the real sources are in a confined environment, (e.g. ducted fans) since the surrounding flow does not require to be artificially bounded and a representative motion is more easily obtained. Difficulties lie more on the measurement side due to the fact that most sound measurements have to be carried out in the flow.

2.0 AEROACOUSTICS IN THE EXPRIMENTAL CONTEXT

In this section, a few concepts of aeroacoustics will be developed in order to unveil the issues of wind tunnel test design and measurements.

2.1 Basic concepts in aeroacoustics

2.1.1 Physical description of aerodynamic sound generation

Aeroacoustics is the field of thermo-mechanics addressing aerodynamic sound generation, that is, generation of sound due to fluid motion. Sound is generated as a by-product of unsteady fluid motion. Unsteady perturbations in a fluid tend to be locally compensated by local reciprocal motion. If a perturbation covers a too large region in a too short time, it cannot be compensated by the reaction of the fluid. This process results in local compressions and dilatations that are transmitted to neighbouring regions *via* a propagation mechanism identified as sound. The tricky part of aeroacoustics is that the local reciprocal motion of the fluid perturbations and its incomplete cancellation are operating at different scales, the latter is a first or even second order effect of the former. They are governed by completely different mechanisms, convection & diffusion for the flow perturbation versus propagation for the resulting sound.

Unsteadiness in a flow may either be inherent to the flow, typically turbulence, or due to a steady flow distortion moving with respect to an object. In the latter case, the object feels an unsteady flow field and reacts accordingly.

2.1.2 Non-local nature, propagation

Contrarily to purely aerodynamic perturbations, sound generated by a flow, as all other sound waves, is a non-local effect that is felt far-off the source region, even outside the flow. Although it is well known, this

aspect of aeroacoustics plays a major role, not only in theoretical, but also in numerical approaches and, as will be seen hereafter, in the design of aeroacoustic experiments.

Since flows always have some spatial extent, acoustic waves have to propagate over some distance through the flow that generated them. Thus sound propagation through flows is an issue that has to be addressed in all aeroacoustic studies, but is often ruled out by appropriate assumptions or simply left aside. For instance, this is the case in most integral aeroacoustic analogies (Lighthill [5], Curle [10], Ffowcs Williams & Hawkings [11] etc.), that propagate sound from its source located in an unsteady flow region, to a receiver, either through a medium at rest or, if a convected Green's function is used, through a uniform flow, which is actually equivalent to a medium at rest *via* a Galilean transform. As will be discussed hereafter and by E. Manoha in the next lecture, this issue may become important in wind tunnel experiments.

2.1.2 Sound, pseudo-sound and evanescent waves

Sound & pseudo-sound

As for other sound waves, propagation of aerodynamically generated sound involves both small density and momentum oscillations of gas particles that are generated by some unsteady forcing in the gas. The main difference is that the forcing is not due to a vibrating plate or string but to the flow itself. In a similar manner as a hard body or a vibrating panel does not need to be compressible to generate sound, an essentially incompressible flow perturbation may also radiate sound waves. This leads to a simplified picture of aeroacoustics that is actually well suited for low Mach number aeroacoustics. The unsteady part of the velocity field may thus be decomposed into an incompressible (divergence free) rotational part and an irrotational compressible part, by the solenoidal field decomposition:

$$\vec{v} = \vec{\nabla} \times \vec{A} + \vec{\nabla}\phi = \vec{v}_t + \vec{v}_a \qquad (1)$$

The former can be attributed to the source, also known as *vortical mode* or *pseudo-sound*, whereas the latter can be identified as sound or *acoustic mode*. Note that this picture also explains the term "hydrodynamic field" that is often used to name the aerodynamic sources.

The two fluctuating velocity components also induce pressure fluctuations. The observed pressure fluctuations can thus be decomposed into:

$$p = p_t + p_a$$

where p_t is the incompressible or *hydrodynamic* pressure and p_a is the acoustic pressure. The hydrodynamic pressure, or pseudo-sound, is felt as sound by a pressure transducer placed nearby the flow or in the flow, but it is not sound: it can be seen as the pressure footprint of the unsteady incompressible fluid motion.

Following Ribner's approach [3], p_t is related to the rotational part of the flow and is solution of the *Poisson* equation:

$$\Delta p_t = -\rho_0 \frac{\partial^2 u_i u_j}{\partial x_i \partial x_j} \qquad (2)$$

whereas p_a is a solution of the wave equation with the hydrodynamic pressure as source term:

$$\Delta p_a - \frac{\partial^2 p_a}{c_0^2 \partial t^2} = \frac{\partial^2 p_t}{c_0^2 \partial t^2} \qquad (3)$$

In these equations, ρ_0 and c_0 denote the density and the speed of sound in the unperturbed gas, $\vec{u}$ the incompressible velocity.

Many approaches in theoretical and numerical aeroacoustics are based on this idea but formulated differently: for instance, Lighthill's analogy clearly assumes the Reynolds stress source term to be incompressible, the compressibility being restricted to the sound field. Similarly, incompressible and unsteady CFD simulations associated with an analogy predict the aerodynamic sound accurately at moderate Mach numbers.

This simple model also tells us that sound generation is linked to local unsteady fluid rotation, that is, to vorticity fluctuations. According to Biot–Savart's law that applies to the incompressible velocity field, the pseudo-sound velocity decreases faster as the inverse of the distance. As a result, pseudo-sound, which scales with the square of the velocity, is only felt within a very short distance of the unsteady flow.

Compressible flows

At higher Mach numbers, flow compressibility effects blur this picture since the flow now carries non-propagating compressible fluctuations that superimpose with the sound waves. The decomposition described above may be generalised to compressible unsteady flows by a multiple scale analysis (see Chu & Kowaznay [12]), which will not be further discussed in the present lecture. Nevertheless, on a local basis, it becomes practically impossible to tell out sound from its source(s) in the flow. One of the issues in experimental aeroacoustics is to develop methods discriminating sound from aerodynamic sound sources.

Evanescent waves

Evanescent waves are non-propagative solutions of the wave equation corresponding to imaginary wave numbers. Subsequently, they are not part of the pseudo-sound, although they decay exponentially away from the source region. They are generated by perturbations whose phase velocity is lower than the speed of sound: in aeroacoustics, typical examples are pressure fields generated by vortical waves in subsonic shear layers and cut-off modes in ducts.

Acoustic near and far field

The propagating part of many sound sources contains a near and a far field component (*e.g* dipoles). The near field component decays with the inverse square of the receiver distance whereas the far field component decays as the inverse of the distance. The criterion separating these two components is the wavelength: if the distance becomes sufficiently large with respect to the wavelength, only the far field remains. Therefore, the near and far field are said to be the *acoustic near field* and the *acoustic far field* respectively. In practical applications, far field conditions are met about one wavelength away from the source that is, between a few centimetres to a few metres in the audible range. As a consequence far field conditions are met in many community noise problems, such as the neighbourhoods of airports, roads and railways. They are always characterised by a lower frequency limit above which far field conditions are met.

Pseudo-sound, acoustic near and far field concepts are illustrated on Fig 2-1: pressure spectra at increasing distances from the trailing edge of a plate at mid-span (32 cm chord and 30 cm span) are plotted with two scalings. The measurements are made with the plate centred in a narrow (13 cm) open-jet wind tunnel (see section 3.1). On the right plot, the $1/R^2$ scaling of the Power Spectral Density (PSD) shows that all results except the nearest measurement point collapse at high frequencies, where far field conditions are reached starting between 200 and 500 Hz depending on the probe distance. On the left plot the $1/R^4$ scaling of the PSD shows the near field behaviour between 20 and 100 Hz depending on the probe distance, except for the nearest. The nearest probe does not collapse with any tested scaling and levels are much higher over the almost whole frequency range except at high frequencies where they become lower: it can be associated to the pseudo-sound of the free shear layers.

This illustration shows that pseudo-sound is restricted to a very short distance around the source or the unsteady flow. The distance of influence is a function of the aerodynamic fluctuation levels and the spectrum is also shaped according to the local aerodynamic fluctuations.

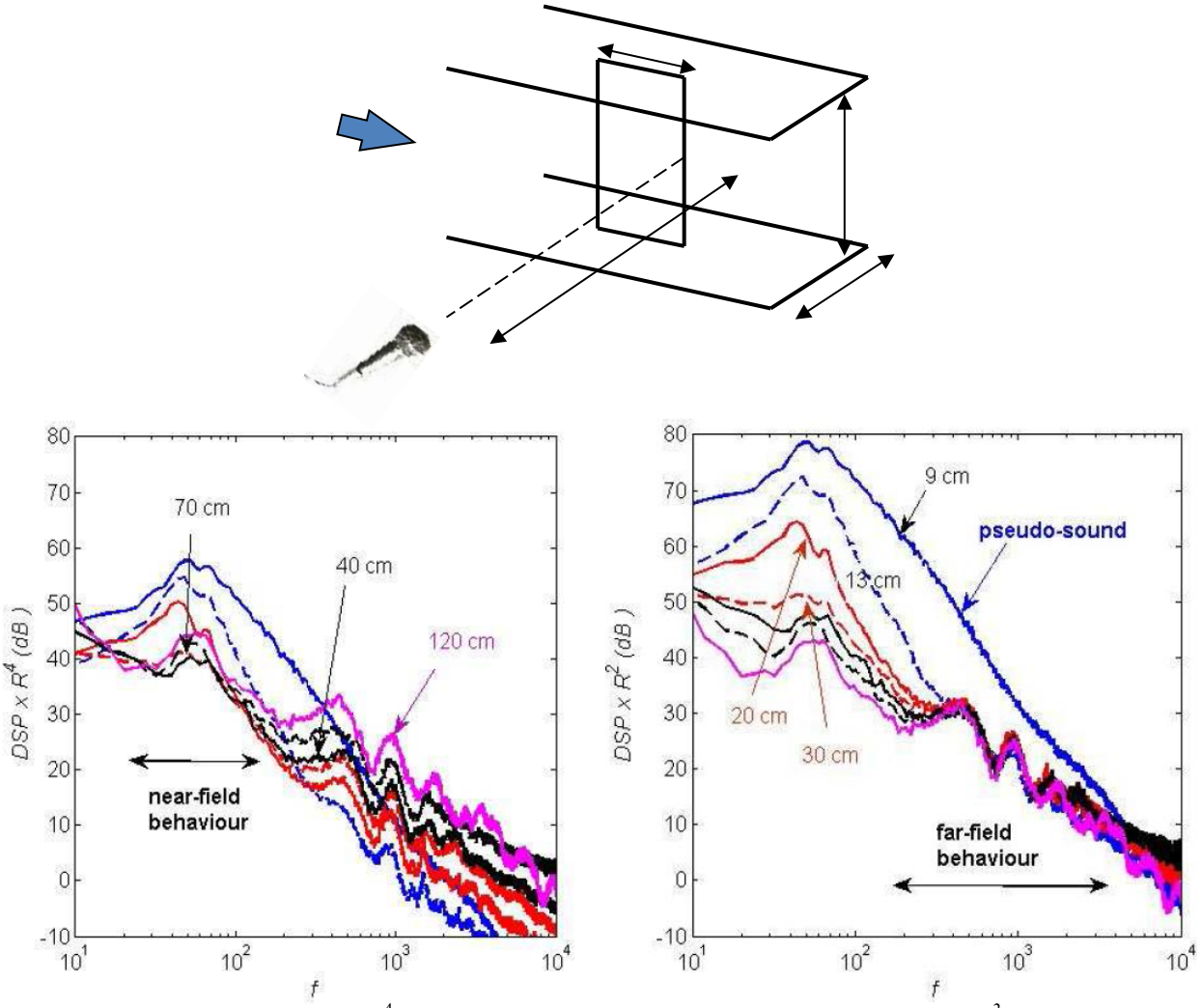

Scaled with $1/R^4$ Scaled with $1/R^2$

Figure 2-1: pseudo-sound, near and far field illustration on flow past a plate blunt trailing edge. Sketch of the set-up (Top). Reduced PSD (arbitrary common reference) of the near-field trailing-edge noise decay (bottom left) and the far-field decay (bottom right). Plate chord 32 cm, span (and end-plates distance) 30 cm. Flow speed 20 m/s. Nozzle width 15 cm, microphone approached normal to the flow direction

2.1.3. Amplitudes

Sound generated by a flow is several orders of magnitudes smaller than the flow disturbances it originates from. For a M~ 0.2 jet of the ECL wind tunnel for instance, the sound power level is about 40 dB below the power level of the aerodynamic fluctuations, that is, 4 orders of magnitude lower. Accordingly, pressure and velocity fluctuations are about 2 orders of magnitude smaller. Depending on the very flow configuration, this sound-to-source ratio might even become much smaller (with a M~0.1 jet, the later drops to 3 orders to magnitude). If sound waves are considered in a perturbed flow region away from their sources, the ratio might even become arbitrarily small. Conversely, if waves are considered in a quiet flow region, the ratio might be more favourable, making noise measurements easier.

Although the example of jet noise is extreme in the sense that it involves only the unsteady motion of turbulent eddies, which is particularly inefficient at low speeds, it is easy to understand that such signal-to-noise ratios make it quite difficult to measure sound within the source regions. When flow perturbations occur in the vicinity of a hard wall, sound generation mechanisms become much more efficient.

2.1.4 Linearity

From the previous subsections, it follows that aerodynamic sound sources are related to non-linear (unsteady) flow perturbations. Nevertheless, the waves generated are linear in many applications, when they are considered outside of the associated source region. Non-linear sound waves are generated in highly perturbed environments (combustions chambers, rockets exhausts,) or by strong discontinuities (e.g. sonic boom), turbulence –shocks interactions, etc.

Linearity / non-linearity is an important issue as the post-processing tools that are applied to experimental results are linear. For instance, coherence is well suited to detect causal links between a sound and its source in the case they are linearly linked, whereas bi-coherence might be appropriate for non-linear links.

At this point it is interesting to note that an appropriate choice of variables might circumvent the non-linearity issue. The wave equation (3) shows that sound pressure is linearly linked to pseudo-sound pressure: the non-linearity is contained in the Poisson equation (2) between the pseudo-sound pressure and the underlying velocity field.

Take for instance the introductory example of the flow past a cylinder: the sound is due to the von Karman vortex shedding aerodynamically scattered by the cylinder surface: the relation between the velocity fluctuations and the acoustic pressure is non-linear but the link between the pressure fluctuations on the cylinder surface and the radiated pressure is linear. The reason is that in this case the aerodynamic pressure fluctuations can be seen as the result on the cylinder wall, of the surrounding non-linear flow perturbations but the conversion of the wall pressure fluctuations to sound is linear. The main source here is not the flow itself, but the motion of the vortical perturbations with respect to the cylinder surface. This argument can be directly transposed to broadband trailing edge noise.

In other applications, incoming flow disturbances may be considered as steady in a convected frame of reference (frozen turbulence assumption). The unsteadiness is essentially due to a quick change of ambient flow conditions due to an inhomogeneity met by the disturbance. This is the case of wake-airfoil interaction noise.

3. WIND TUNNEL EXPERIMENTS IN AEROACOUSTICS

In the previous section we quickly mentioned some characteristics of aerodynamic sound generation that might in some way impact the design and exploitation of aeroacoustic wind tunnel experiments. Here we will discuss what experimental set-ups are classically used and how they address or not the issues raised by aeroacoustic investigations. One major difficulty that appears in aeroacoustics is that aerodynamic sound sources cannot be tested without the flow that generates them: this truism actually makes it very difficult to characterise precisely many sources encountered in aeroacoustics for the simple reason that they cannot be unambiguously separated from the background noise of the surrounding flow and from related installation effects. Solutions often consist of blending “reasonable assumptions” (e.g. uncorrelated sources) with data processing techniques (decontamination, causality techniques..).

3.1 Open-jet experiments

3.1.1 Description

Open-jet experiments are very popular set-ups in the aeroacoustic community: the reason is that they offer a convenient way to investigate both the aerodynamic and the related sound field. They consist ideally of a jet flow that develops from a nozzle into an anechoic room mimicking an unbounded region of fluid at rest. Such a facility is currently being built at ISAE-SUPAERO in Toulouse for airframe noise applications but many other exist throughout the world (especially in the US) and in particular in Europe. To name a few: DLR – Braunschweig (similar test section as in Toulouse), ECL (smaller test section but larger Mach numbers, that has been recently upgraded), ONERA – Cepra 19, (very large facility)... A number of wind tunnels are built in semi-anechoic rooms for ground transportation issues such as FKFS – Stuttgart, S2A – St

Cyr, and among the most recent ones, there is the new Mercedes Wind Tunnel in Sindelfingen.

Two cases have to be distinguished:

- either the jet itself is investigated, in which case there is no real alternative to choosing an open-jet configuration and all aerodynamic sources are part of the investigated process. Ideally the nozzle is placed away from the back wall to reduce its influence onto the entrainment and to allow for sound measurements in the rear arc. The major remaining difficulty is to avoid influencing the jet flow and sound by the experimental apparatus, especially if simultaneous aerodynamic and acoustic measurements are to be performed. An example is shown on Fig 3-1 for 2 jets developing downstream of a diaphragm and downstream of a multi-perforated plate respectively at subsonic speed (subcritical pressure ratio) [13]. The acoustic results agree perfectly well with spectral models [14] showing that each 'jetlet' leaking through a perforation behaves as a jet and the whole assembly of mini-jets behaves as a global jet.

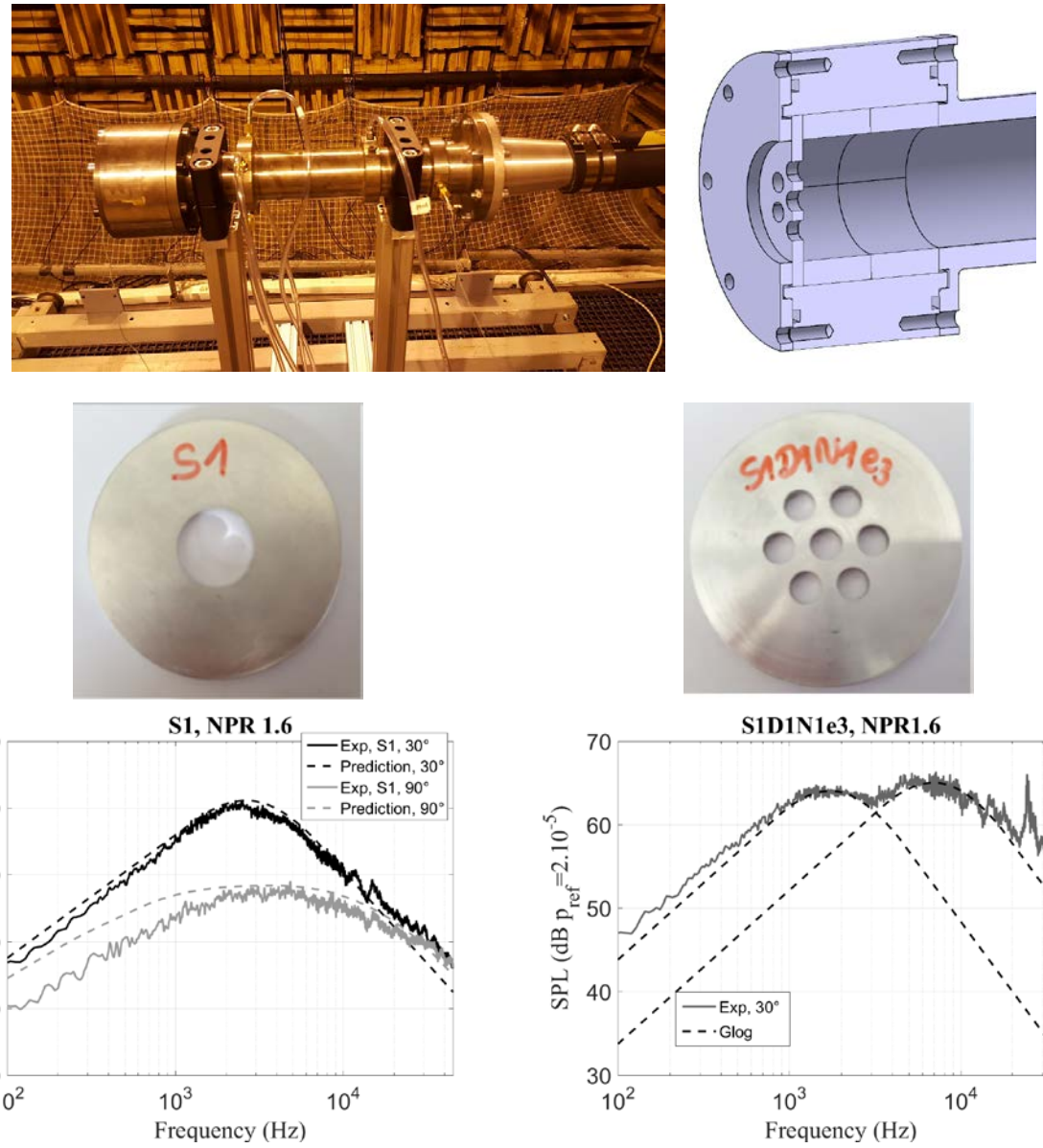

Figure 3-1: Jet with diaphragm nozzle (left) and multi-hole nozzle (Right) at iso-cross-section pressure ratio 1.6: the spectra agree with self-similar model of Tam et al. [14]

- or the source is not the jet itself, but a body such as an airfoil or any other mock-up whose aeroacoustic

properties have to be determined. The latter is generally supported by one or two plates that may or may not have a connection with the original problem. The mock-up is placed into the potential core of the jet where the flow is uniform and has a vanishing turbulence level (less than 1% typically). If interaction noise between such a body and impinging flow disturbances is to be examined, this is often achieved by adding a turbulence grid upstream of the nozzle: thus turbulence intensity and length scales of the incoming disturbances can be tuned. Another way to generate incoming disturbances is to place another body upstream of the mock-up, as was done for instance by Jacob et al. who placed a circular cylinder one chord upstream of a NACA0012 airfoil in the potential core of a jet [15] (see Fig 3-2) or by M. Gruber who placed an airfoil with a wavy leading edge into the wake of another airfoil with a serrated trailing edge [16].

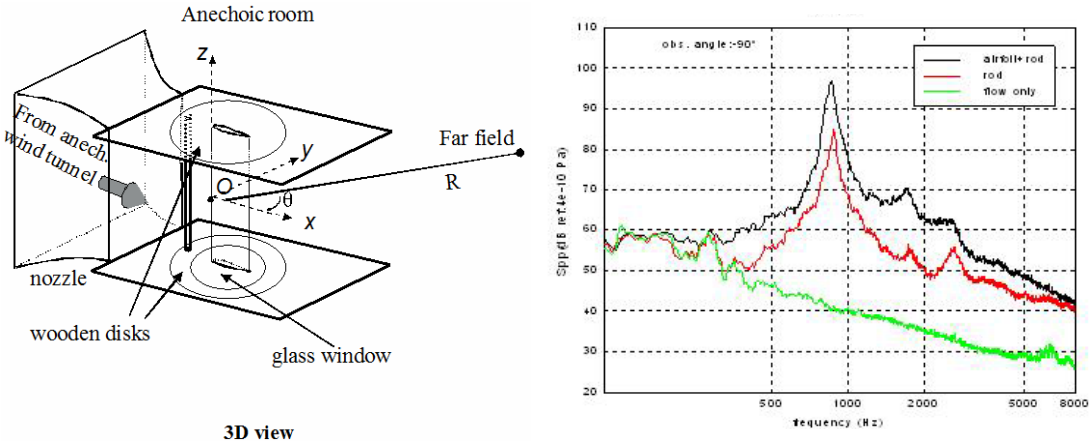

Figure 3-2: Rod-airfoil experiment at U=72 m/s: sketch (left) and far field noise spectra at 90° to the flow direction (right): background noise by guided jet (green curve), Rod only (red curve), Rod-airfoil (Black curve).

3.1.2 Advantages of open-jet experiments

Open-jet experiments do have many interesting features provided they are conducted properly.

In particular they offer a very convenient and natural way to separate sound from pseudo-sound since they take advantage of the propagative nature of sound and the local nature of pseudo-sound by including a sufficiently large medium at rest around the flow. Indeed, only the sound waves remain away from the flow. If the surrounding anechoic medium at rest extends over more than a wavelength from the flow boundaries, sound measurements are not only free from pseudo-sound but are also ensured to contain only the acoustic far field. Hence the far field directivity of an aerodynamic sound source can be characterised just as any other source placed into an anechoic room. For similar reasons microphone arrays facing the flow test section, may help localising the sources both in space and frequency (see lectures 4 (L. De Santana) and 5 (A. Finez) of the present lecture series).

In addition, the source region can be characterised in the same flow configuration as the far field. This is crucial for benchmark experiments that are to be compared to numerical simulations of the flow and sound field.

At this point it should be underlined that some well-known benchmark configurations do not fulfil this requirement: indeed in some cases, aerodynamic measurements are carried out in a closed test section wind tunnel whereas the acoustics measurements take place in open flows. The reasons for such surprising choices are numerous and may be justified in some cases (see section 3.2.3). Nevertheless, for benchmarking purposes this approach leaves an ambiguity as to the similarity between the two configurations, that requires

additional investigations in order to be removed. Therefore, dual set-up tests should be avoided if possible.

Another reason advocating for full studies in open-jet configurations, is that simultaneous aerodynamic and far field sound measurements are possible, provided that the aerodynamic probes do neither generate significant levels of spurious noise in the spectrum of the actual source nor interact in any other way with it. This aspect is difficult to overcome in general and will be addressed in the next section as well as in other lectures of the present course. However, at this point let us just mention that some aerodynamic measurement techniques are better suited than others for joint aerodynamic and acoustic measurements.

3.1.2 Issues for open-jet experiments

Besides design requirements of the facility that will not be further discussed here (anechoic room large enough to reach the far field conditions in the desired frequency range, flow facility free from wind tunnel blower or compressor noise etc..), there are some questions that have to be addressed when measurements are carried out in such a facility.

Jet spreading

A free jet expands very rapidly downstream of the nozzle due to the diffusion of shear layer mixing and the resulting short size of the potential core (about 4-6 equivalent diameters downstream of the nozzle). In order to have a large enough zone of quiet flow to place the mock-up, only the first 2 diameters can be exploited. Thus the sound generated by the mock-up might interact with the nozzle lips modifying its free field directivity. When the jet is guided as shown on Fig. 3-2, the mixing surface is reduced and the potential core length increases, especially along the guiding plates where boundary layers affect the potential flow only over a thin layer on each plate. In the case shown on Fig 3-2, the rod-airfoil system has an aspect ratio that is compatible with the potential core evolution (small size in the direction of the free shear layers, longest size in the direction of the boundary layers). The potential core issue should always be at least considered to avoid unlucky positions of the mock-up.

Background noise

In the case, the jet is not specifically investigated but only acts as the flow surrounding an aeroacoustic source of interest, several questions arise:

- the jet noise should not cover the sound radiated by the actual source, which can be achieved in two ways: either the source is much louder than the surrounding jet or the maximum jet noise is reached in a frequency range that differs from the source : both conditions are met in the case of the rod-airfoil study illustrated on Fig 3-2, for which the jet emits around 60 Hz, that is far below the frequency range of the rod-airfoil configuration ([400 – 4000 Hz]. In this example the rod, which acts here as a vortex generator with respect to the airfoil interaction noise mechanism, radiates 5 to 15 dB below the airfoil noise: thus the pure interaction noise can be computed by a spectral difference between the rod+airfoil far field spectrum and the rod alone noise spectrum although the 2 sources cover the same frequency domain. Another example is shown on Fig. 3-3: a backward facing step is placed under a wall jet far downstream of the jet mixing region [17],[18]. The step height is $h = 4$ cm, the jet width in the cross-stream direction is 5 cm with an aspect ratio 10 and the velocity is 140 m/s. The axial source localisation sketched on plot (a) is carried out both with (c) and without step (b). In this example, the jet noise is not only lower than the step noise for a given frequency but it is also centred at a different position: here the source localisation provides useful information to discriminate the two sources. It can help interpreting the far field results.

Flow effects on propagation

Another important aspect to be taken into account for when aeroacoustic sources are placed into a free shear flow, is the influence of the flow onto the propagation. There are 3 possible effects of a turbulent shear flow

onto propagation:

- Waves are convected as they propagate from their source to the free boundary
- Waves are refracted by the free shear layer at the boundary
- Wave fronts may be distorted by the flow turbulence.

The first two effects modify the directivity and the amplitude of the radiated sound: they will be further discussed in the second lecture (E. Manoha). The influence of turbulence is a cumulative effect. It leads to slight wave front rippling and small random phase shifts and remains negligible in most wind tunnel experiments, except for very high frequencies in very large wind tunnels and/or at very shallow observer angles.

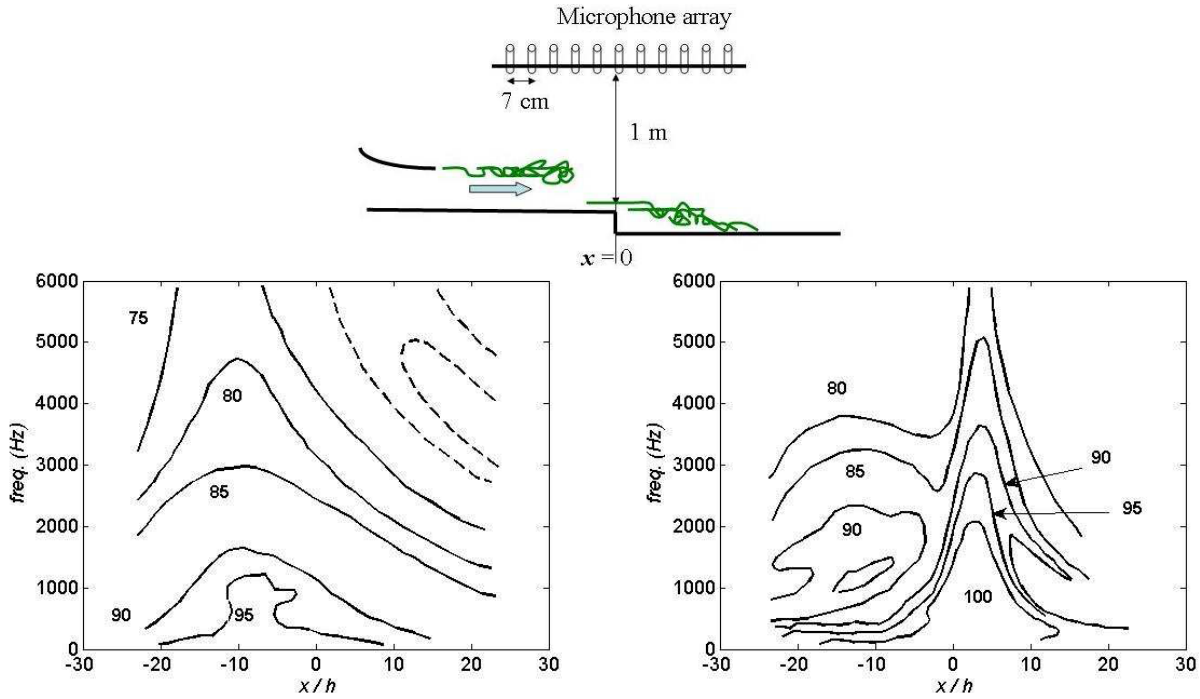

Figure 3-3: Backward facing step under a wall jet at 140 m/s. Sketch of the set-up (top plot). Axial distribution of the source intensity spectrum: jet only (left) and jet + step (right). The axial source distribution is made non dimensional by the step height *h* [17],[18].

Deviation by model

Another issue to be aware of when designing an open-jet experiment is that the model might deviate significantly the jet. This becomes a crucial issue in aeroacoustic open-jet experiments since the jet might be deflected into the room walls and damage the foam wedges. If the model is for instance a heavily loaded airfoil (high camber and/or angle of attack), the jet deviation might become important. In a recent experiment that will be further discussed in the 11th lecture of the present lecture series, the authors observed a 7.5° deviation that was about half of the angle of attack. Without further care, the jet would have damaged the anechoic room.

One way to compensate this deflection is to deviate the incoming jet flow by the opposite angle: in the case mentioned above, the duct leading to the jet nozzle was bent two meter upstream of the nozzle by 7.5° to the left for a deflection of 7.5° to the right (see Fig. 3-4): as a result the flow downstream of the airfoil was

directed towards the exit aperture of the anechoic room and did not hit the wedges.

Another way to mend this deflection problem is to oversize the jet section with respect to the mock-up: this approach is suited for large flow facilities.

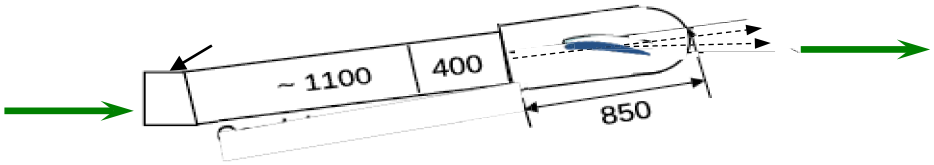

Fig 3- 4 Bending the flow upstream of the nozzle to compensate downstream deflection (EU Project PROBAND and Jacob et al[23])

Installation effects

Installation effects should be taken into account as in all acoustics experiment: all apparatus, supports, even microphones supports may diffract or scatter sound waves in some way. The difficulty with aeroacoustic experiments is that the flow facility itself may distort sound waves. An example is shown on Fig. 3-5 (Moreau & Roger (2009) [19] & Schram), where the lips of a nozzle modify the directivity of Tollmien-Schlichting waves radiated by a NACA0012 airfoil at 0° angle of attack in a 20 m/s flow. The chord is 0.1 m and the frequency is around 2.5 kHz. The directivity predicted by Amiet's model is similar to that obtained by a Boundary Element Method computation of equivalent trailing edge sources diffracted by the airfoil modelled as a flat plate, but differs from the measurements. Since the airfoil is in the vicinity of the nozzle, it diffracts the sound. Applying to the free field predictions, a directivity correction obtained by taking into account the nozzle side lips in a second simulation, explains the additional lobe found experimentally. This exercise shows that geometrical details of the flow facility may have a significant impact onto the acoustic results.

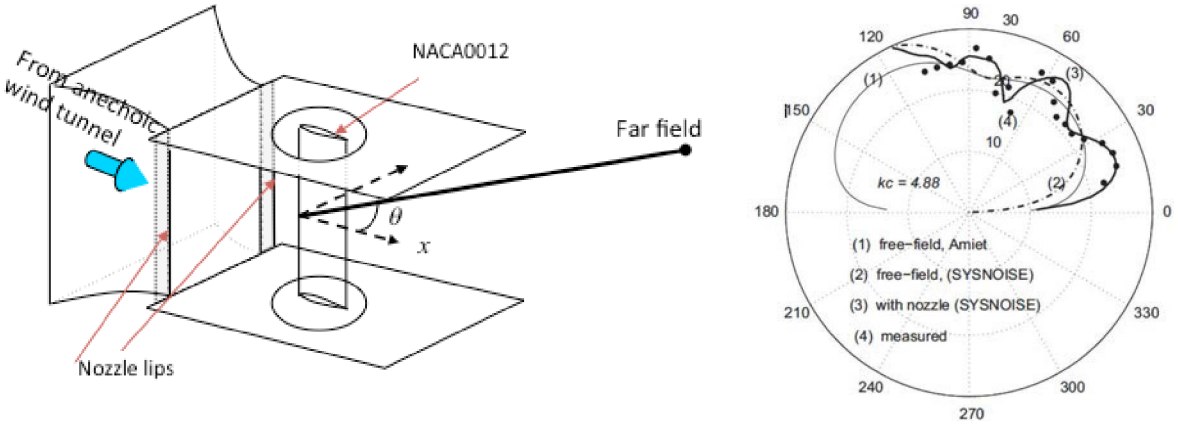

Fig 3-5: Measured and computed directivities for TS wave radiation. Experimental set-up (left). Directivity compared to anamytical model, simulations with /without the nozzle lips (right). Levels in relative decibels. NACA0012 airfoil at $U_0 = 20$ m/s and 0° angle of attack [19].

3.2 Closed section wind tunnel tests.

There are several types of closed test section experiments, namely experiments mimicking an original duct flow situation, experiments reproducing free field or semi free field configurations with a uniform flow or a wall flow. Finally, if the duct is finite and open ended, the inlet/outlet may be placed into an anechoic room, allowing for far field measurements. If the flow is obtained by suction, the intake flow is quiet and might be used for sound measurements. Open ended configurations are typically be obtained with ducted turboengines

such as in the ANECOM (ACAT) wind tunnel facility for 1/2-scale fan rigs, or more recently, the PHARE 2 wind tunnel for 1/3 scale fan rigs at Ecole Centrale de Lyon.

3.2.1 Walls and duct modes

When a sound wave propagates in a duct, its shape is imposed in all cross-stream directions at a finite distance by the duct walls. As a result, the sound is a superposition of modes with standing wave patterns in the cross-stream direction(s) and/or periodic azimuthal phase oscillations. Along the duct axis, these modes may be propagative (cut-on) or damped (cut-off), depending on the mode order and the frequency. As a result, sound measurements come down to modal analysis.

For a rectangular duct with cross-sectional dimensions a, b in the x and y directions respectively, whose axis is aligned with the z −axis, the complex pressure field of an isolated mode may be written:

$$\hat{p}_{n,j}(x,y,t) = \cos\left(\frac{2n\pi x}{a}\right)\cos\left(\frac{2j\pi y}{b}\right)e^{i(\omega t - k_z z)}$$

where $A_{n,j}$ is a complex amplitude whereas the axial wavenumber k_z (that should be labelled $k_{z,n,j}$) is given by the dispersion relation:

$$k_z^{\pm} = -\frac{M_0 k}{\beta^2} \pm \frac{1}{\beta^2}\sqrt{k^2 - \beta^2\left[\left(\frac{n\pi}{a}\right)^2 + \left(\frac{j\pi}{b}\right)^2\right]}$$

where M_0 is the axial-flow Mach number and $\beta^2 = 1 - M_0^2$. The corresponding modal cut-off frequency (vanishing axial wavenumber) is obtained directly:

$$f_{n,j} = \beta\frac{c_0}{2}\sqrt{\left(\frac{n}{a}\right)^2 + \left(\frac{j}{b}\right)^2}$$

Each mode is either cut-off below the cut-off frequency or cut-on above. For each lateral mode there are two axial wave numbers ($= 2$ roots of the dispersion relation) $k_z^+$and k_z^- corresponding to downstream propagating (or damped) waves and upstream propagating (or damped) waves. A duct sound field is general a weighted sum of all these modes and writes as follows:

$$\hat{p}_{n,j}(x,y,t) = \sum_{n,j} A_{n,j}^{+}\hat{p}_{n,j}^{+}(x,y,t) + A_{n,j}^{-}\hat{p}_{n,j}^{-}(x,y,t)$$

where $A_{n,j}^{+}$ and $A_{n,j}^{-}$ are the complex amplitudes of downstream and upstream propagating/damped waves, respectively. They are determined by the source. In particular for a single source in a smooth infinite duct there are only "+" modes downstream of the source and "-" modes upstream of the source. In general both types of modes exist (muffler, expansion/contraction, reflection by open end...)

Since the cut-off frequency is increasing with the mode order, at a given frequency, the number of modes in this sum is finite far enough from the source(s), but the number of modes contributing to the field and the radiated sound power increases with the sound frequency: this gives a complex structure to high frequency waves in ducts.

For circular, or annular ducts, the analysis is quite similar with a bit more complicated algebra (first and second kind Bessel functions) and structural change due to the axisymmetric geometry that imposes 2π −periodicity to the field and a simple modal structure for the radial evolution.

These few lines set the theoretical background that guides all aeroacoustic studies in closed wind tunnels. We will now quickly list the main types of aeroacoustic duct experiments that one may encounter in the literature.

3.2.2 Ducted sources

When the original aeroacoustic problem is that of a ducted source, the experimental configuration is conceptually rather straightforward. Consider for instance a ducted fan: a test configuration reproducing the fan and the duct or a part of the duct, possibly downscaled to a laboratory-friendly size will do the job. In more fundamental experiments, one often prefers simplified duct geometries (rectangular, cylindrical, annular) in order to obtain analytic expressions for the duct modes and the tailored Green's function (as illustrated on Fig. 3-6)

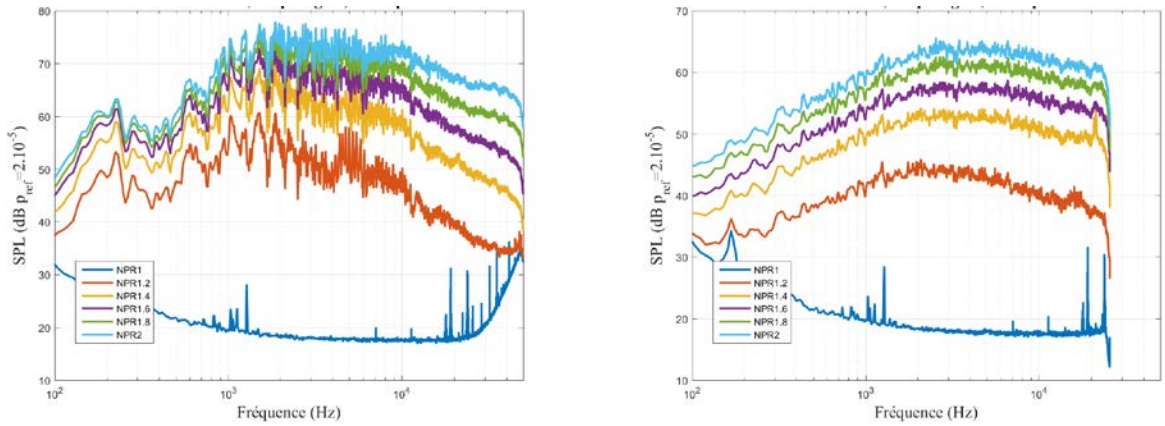

Diaphragm S1 mounted into a finite length duct **Diaphragm S1 opening into free space (see Fig 3-1)**

Fig 3-6: Influence of duct modes onto a jet leaving a diaphragm at various pressure ratios (NPR). From bottom to top: NPR= 1 (no flow), 1.2; 1.4; 1.6; 1.8; 2.

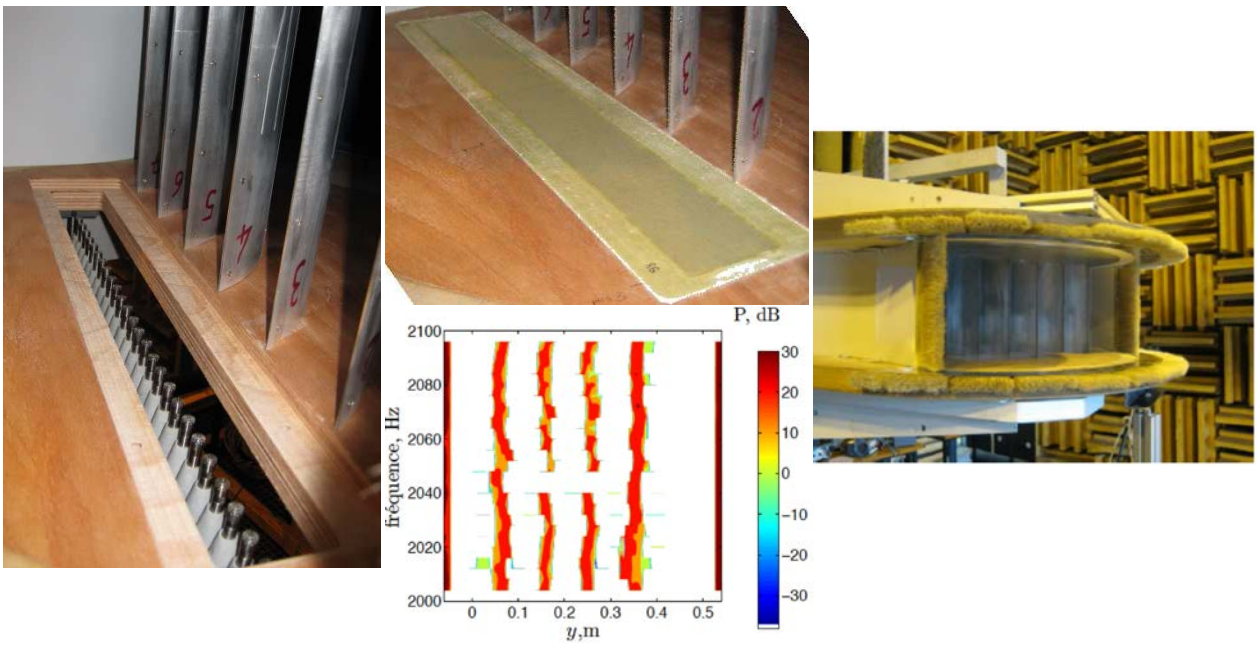

Array of 26 microphones beneath the "casing" plate downstream of the cascade trailing edges **View of Kevlar Liner and typical localisation result at 60 m/s – 2 kHz with CLEAN-SC** **View of the cascade opening into the ECL anechoic room**

Figure 3-7: Example of wall mounted localisation array in semi-open test section.

Similarly a duct with a singularity such as a diaphragm, a sudden expansion or contraction might be investigated *as is*. In such configurations the effects of the duct onto the flow, the sources and the waves they

emit, are part of the initial problem. The main difficulty is to carry out measurements in these confined environments. Although they are not always easy to address, aerodynamic measurement issues in ducted flows have been tackled for many years and even optical measurements can be carried out successfully if the ducts are equipped with glass windows. The difficulty lies more on the acoustic side, since flow and sound are intimately mingled in duct flows (pseudo-sound & sound). Details will be discussed in the lecture about microphones (M. Roger) and in the lecture dedicated to in-duct measurements (M. Abom). Let us just mention several types of measurements that may provide acoustic data: far field microphone measurements through a duct inlet or outlet if available (both source localisation[20] and directivity/power see Fig- 3- 6, by Laffay - ECL), wall pressure measurements or free flow microphones with turbulent screens or nose cones (see M. Roger's lecture n°3) to identify duct modes in quiet flow regions upstream of the sources, advanced circular microphone array measurements with appropriate decontamination and modal analysis (see lecture n°9 of the present series by M. Abom) and last but not least, planar microphone arrays installed in the walls some distance behind flush-mounted Kevlar or wire-mesh liners (see following lectures). An example of the latter is given in a semi-open cascade flow on Fig 3-7 [21]. A microphone array is mounted into the spanwise bounding plate slightly downstream of a cascade trailing edge section and the array is focused on the mid-span trailing edge line. To finish this section, let us mention another type of duct experiments, in-duct characterisation of liner impedance that will be presented in lecture n°10 by Y. Auregan.

3.2.3 Free source placed inside a duct

Sometimes sources that are usually observed in free flows are placed in closed test section ducts as already mentioned in section 3.1.2.

The reasons for such surprising choices are numerous: in closed test sections that are large enough with respect to the mock-up, uniform flow conditions cover a large part of the flow (except the duct boundary layers and the wake of the mock-up, the latter being part of the study): in particular the interaction with the mock-up or the mock-up support with shear layers are replaced by the interaction with much thinner boundary layers; a closed test section makes it easier to support the mock-up. Thus the channel flow might be closer to uniform flow conditions experienced during a flight or assumed in a computation; if it is equipped with glass windows, a closed section facilitates the operation of optical probes as the distance to the flow is well-defined; if the test section is inserted in a closed loop wind tunnel, parameters such as flow temperature are more stable and may even be controlled; the apparatus for aerodynamic measurements often includes large equipment and carriage displacement that is not easy to remove from the wind tunnel in open-flow configurations and is likely to flaw free field sound measurements: in a clean closed test section, the conditions for wave propagation are indeed influenced by modes but these may be predicted and de-convoluted when the signals are post-processed, which is not the case when complex apparatus is placed into an otherwise anechoic environment. Finally some wind tunnel operators do not always have the choice as open-jet facilities are not available everywhere or the ones available might not be suited for a specific experimental study. An example is shown on Fig 3-7. The cascade loses its periodicity condition if it is placed in an open-flow: therefore the flow is guided along the 7 blades of the cascade as shown on the right plot of the figure. In order to identify the trailing edges as sources, localisation techniques were also applied. The figure shows the hardware and a typical result of the array measurement campaign.

3.2.4 Dual wind-tunnel tests

To circumvent the difficulty of running one-shot wind tunnel experiments in open flow configurations, and having to remove large equipment from the room when the acoustic measurements are to be carried out, or to run full tests in closed test sections and having to treat the acoustic data accordingly, many experiments are carried out in dual wind tunnel test campaigns: the aerodynamic data is collected from a closed test section wind tunnel whereas the sound measurement campaign is performed in an open-jet facility. For instance two celebrated AIAA benchmark tests have been documented using a dual approach, the tandem cylinder test case (detailed aerodynamic measurements in the closed test section BART facility and acoustic measurements in the QFF open-jet facility at NASA Langley) and the landing gear model test case Lagoon

(detailed aerodynamic measurements in the closed test section F2 facility at ONERA – Fauga-Mauzac and acoustic measurements in the CEPRA 19 open-jet facility at ONERA-Saclay).

Carrying out a test in several facilities or in several flow configurations requires special care such as defining common measurement points for verification purposes, that will be detailed in the lecture n°2 by E. Manoha. Nevertheless some ambiguity as to the interchangeability of the flow data always remains.

3.3 Hybrid Wind tunnels

Let us finish this section by mentioning two types of hybrid wind tunnels and illustrating them with a few examples

3.3.1 Open channels

One of the difficulties encountered with open-jet experiments is the limited extent of the potential core region. As already mentioned, this can be improved by taking advantage of the mock-up support to guide the jet with one or two support plates. Additional sources due to the plate-end wakes can be considerably reduced with noise supressing devices such as brushes as can be seen on the cascade holding plates on Fig. 3-6-right. In some cases the "jet flow" is even guided by 3 plates: this was done for the backward facing step experiment illustrated on Fig 3-3: indeed the challenge of this experiment was to maintain a high speed flow over the backward facing step that had to be placed sufficiently far downstream (20 nozzle thicknesses in the case shown on Fig 3-3). By guiding the wall jet on its sides, the spreading was limited to only one direction, namely the direction normal to the wall containing the step. As a result, the potential core reached far downstream and the maximal velocity (140 m/s in the case shown on Fig 3-3) could be reached above the step.

The difficulty arising with such a configuration is that the "free" jet is not that free anymore but becomes a 3-sided channel, which gives rise to duct modes. As a result interference patterns appear in certain directions of the far field as shown on Fig 3.8.

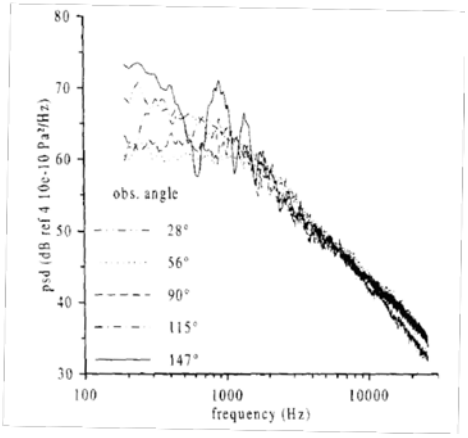

Fig 3-8: Interference pattern in the far field of a guided rectangular wall jet past a backward-facing step [17]: 140 m/s – nozzle thickness e= 5 cm – Step height h= 4 cm Obs. angle with respect to downstream direction

Acoustically transparent ducts

In order to circumvent the open-jet and the closed test section related difficulties, some aeroacoustic wind tunnels use ducts with Kevlar walls (e.g. Stability Wind tunnel at Virginia Tech at Blacksburg - see left plot of Fig 3-9 - from Virginia Tech's Website) or other materials (Nylon cloth and Wire mesh at ECL, see the right plot of Fig 3-9) and to place these soft ducts into an anechoic room. The idea is to guide the flow aerodynamically and especially to reduce the turbulence with respect to free shear layers without confining

the sound. This both avoids the presence of duct modes and allows for far field measurements. The acoustic transparency reached with these materials is excellent (about 1 dB attenuation over a wide frequency range is possible), but they are also partially permeable to the flow and its fluctuations. This approach is particularly well suited for acoustic array measurements and for near-to-far field causality measurements. However, fluctuations at high frequencies due the micro-jets across thewalls, may generate additional broadband noise. Best results are achieved if the mock-up does not have a significant blockage effect (not as on Fig 3-9 right) and the flow remains parallel to the walls.

Virginia Tech transparent wall duct (Kevlar)

ECL Transparent Wall duct (Nylon)

Fig 3-9 Examples of acoustically transparent ducts for aeroacoustic studies

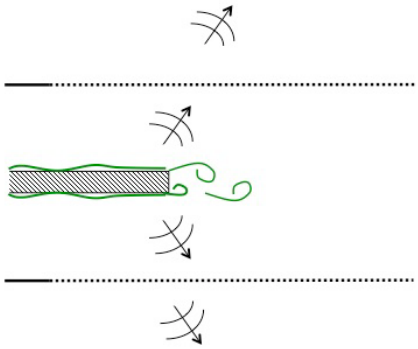

Sketch of the transparent wind tunnel: transparent walls represented by dotted lines

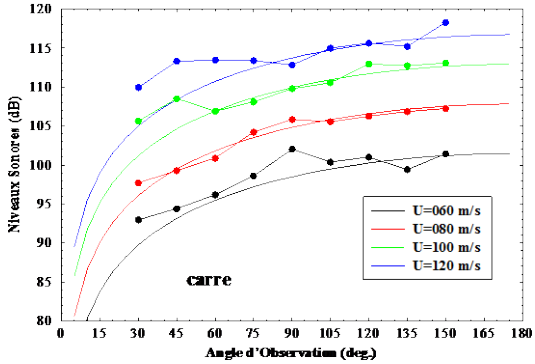

Experimental and theoretical far field directivities (Blake's model [22]). Angle with respect to downstream direction

Fig 3-10: Acoustically transparent test section in an anechoic room: far field result

Moreover, the wall roughness increases the boundary layer thickness that in turn generates an adverse pressure gradient increasing a flutter tendency: this has to be taken into account when designing the liner panels: if Kevlar is correctly installed it flutters much less than the older Nylon solution. Fig 3-10 shows a successful application of such a channel to the noise measurement of the flow past a blunt trailing edge. Note that here the far field directivity is quite accurate compared to Blake's model [22]: this is partly due to the fact that the source, which is tonal, peaks out of the background noise and is thus less prone to distortion.

Following this quick and certainly incomplete review of aeroacoustic testing strategies, let us now say a few words about the measurement issues in aeroacoustics.

4. AERODYNAMIC MEASUREMENTS FOR AEROACOUSTICS

In the previous section we went through a few issues about aeroacoustic wind tunnel testing, according to the chosen flow configuration. We will now discuss about some specific requirements and features of measurements in the aeroacoustics context. As acoustic measurements in a medium at rest do not drastically change when the source is aeroacoustic (provided that the chosen flow configuration makes such measurements possible), we will not cover this aspect in the present lecture. Thus we will focus on flow embedded measurements, both aerodynamic and acoustic, and also mention joint flow and far field measurements, as they are really specific to aeroacoustics.

4.1 Flow data required for aeroacoustics

In this section, we will list some important aerodynamic features that have to be measured during aeroacoustic wind tunnel tests.

As mentioned in the introduction, there are various types of aeroacoustics experiments, “fundamental” experiments that are meant to unveil a new physical mechanism of aerodynamic sound generation, benchmark experiments that are designed for CFD validation, and industrial rig experiments whose role it is to measure parameters that cannot be obtained on full scale objects in their environment. The design and measurement requirements of the latter are essentially governed by the need for representativity with regard to the full size object in operation. This topic will be addressed in more detail by E. Manoha in lecture n°2.

Let us focus on the first two types of experiments: in many situations the two aspects, that are understanding the physics of sound generation and providing benchmark data for CFD-CAA codes or models can be covered by the same set-ups.

Generally speaking, all aeroacoustic experiments, just as purely aerodynamic experiments, require an extensive description of the mean flow parameters as well as of the rms values of the turbulent velocity fluctuations.

In particular, in the purpose of benchmarking, the oncoming flow should be thoroughly characterised at least in one upstream cross-section that may be used as inflow boundary of the CFD domain.

The mean flow characterisation should also allow checking that the aeroacoustic source whatsoever is located in the part of the flow where it is supposed to be located, say, the potential core of the open-jet.

These measurements can be achieved with any measurement technique used in aerodynamics if sound measurements are not carried out simultaneously (HWA, LDV, PIV, Pitot probes).

4.1.1 Classical unsteady flow statistics

In the first section, it was underlined that sound is generated by the fluctuations of the vortical disturbances in a flow or by the convection of a steady disturbance past a flow inhomogeneity: in both cases, unsteadiness is part of the game and this should be targeted by appropriate measurements.

Once the rms values of velocity or pressure fluctuations are known, other more detailed flow statistics of the unsteady flow are required, both as input for analytical models and for benchmarking unsteady CFD codes.

For instance, airfoil noise models require not only convection velocity information but also the spanwise coherence length and either turbulent velocity spectra (turbulence-airfoil interaction) or wall pressure spectra (trailing edge noise). For traditional jet noise models, space-time velocity correlations need to be measured in the mixing region.

Aerodynamic velocity spectra are easily and quite accurately obtained from one-point measurements (HWA or LDV): such information might to some extent be sufficient for modelling purposes. For benchmarking, this is a minimum option as unsteady CFD resolves more and more complex flows with increasing time and space resolution. Spectral charts over a whole region are more difficult to obtain experimentally for the velocity components. However, thanks to continuing progress in time-resolved PIV hardware, it is now possible to obtain whole 2D-maps of the low frequency end of the spectra with improving accuracy [23]: on Fig 4-1, the measurements obtained in a tip clearance vortex (see lecture n°11) are accurate up to about 1 kHz although the sampling frequency is 7 kHz: according to the slope of the spectra above 1 kHz, the discrepancy is unlikely due to a sampling aliasing. It is believed that the error comes rather from the complex environment (light reflections). It can be expected that the high frequency limit of this technique will increase during the next decade or so, putting time and space resolved flow descriptions within reach.

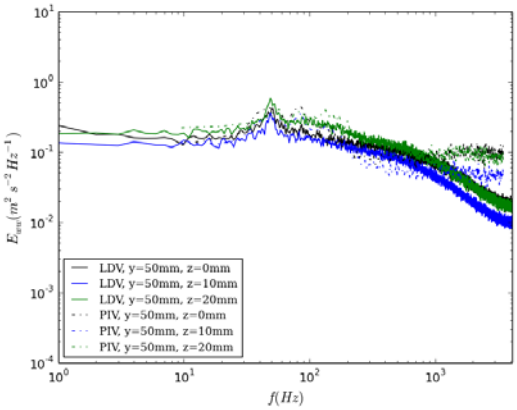

Fig 4-1: Comparison of Spectra obtained from LDV and time-resolved PIV at 3 positions in a tip leakage vortex [23] (see also lecture n° 11 by M.C. Jacob)

As far as wall pressure measurements are concerned, the feasibility often depends on the available room for pressure sensors, their characteristics (sensitivity, dynamic range, diameter, installation, calibration). This matter will be thoroughly discussed in the lecture n°3 by M. Roger.

4.1.2 Two-point measurements

Other statistics of the unsteady flow can be obtained from two-point measurements:

Two-point correlations indicate the causal link between the physical quantities that are measured. They are classical in experimental turbulence, but are nevertheless useful in aeroacoustics as many aeroacoustic responses depend on the size of the structures they originate from.

An important parameter for aeroacoustic modelling is the coherence between two quantities taken at two points x and y in a flow: the coherence $\gamma_{x,y}^2$ is a non-dimensional function of the frequency (whose values are comprised between 0 and 1) that is proportional to the square modulus of the cross-spectrum between the two signals for a given frequency. Moreover, still for a given frequency, the integral $\ell(\omega)$ of its square root $\gamma_{x,y}$ over all the possible distances between the two measurement points in a given direction, is the frequency dependent correlation length, which relates the size of the structures to their frequency in that direction.

More generally, coherence between some physical information at two points in space, tells us that there is a causal (linear) link between the phenomena observed at these two points. This implies that the two points feel the effect of a common physical phenomenon. It may measure the eddy size or hint at a propagation/convection between the two points.

Another important information of the cross-spectrum function is the phase: measuring the phase shift between two points of the pressure field gives access to the local convection velocity or may show evidence of propagation or provide convection velocity the associated eddies.

An example of the spanwise coherence and coherence length as well as the convection velocity computed from a phase spectrum is illustrated on Fig 4-2. Data is obtained from wall pressure measurement near a NACA5510 trailing edge placed at 15° angle of attack into a 72 m/s flow.

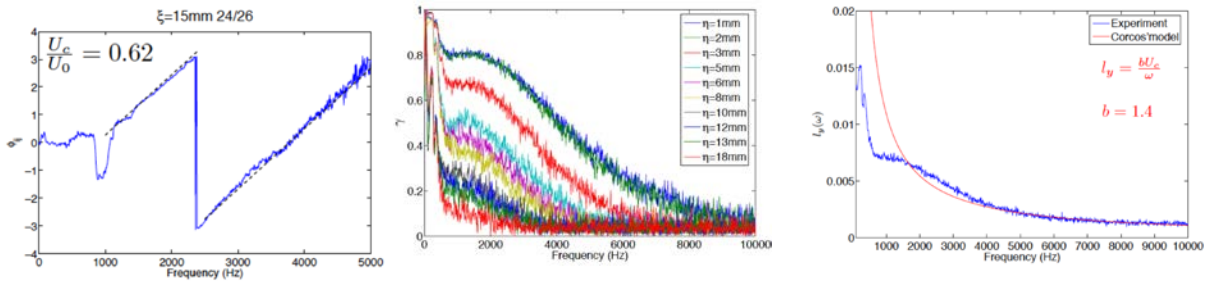

Phase shift between two neighbouring probes

Coherence for several spacing between two points

Correlation length: measurement versus Corcos' model (exponential decay)

Fig 4-2 Phase and coherence from pressure measurements on the suction side of an airfoil at 72 m/s. The frequency dependent correlation length is in good agreement with the model for higher frequencies and the computed phase velocity coincides with the usually assumed value [24]

4.1.3 Advanced unsteady measurements

Other useful information that can help understanding unsteady flow physics relies on advanced techniques.

Phase locked measurements

Such measurements are related to periodic flows like wakes of a rotor, vortex shedding downstream of a cylinder or a cavity lip. They consist of starting a new measurement at each occurrence of the periodic event. These measurements can then be used to compute ensemble averages, of time signals, PIV snapshots etc..

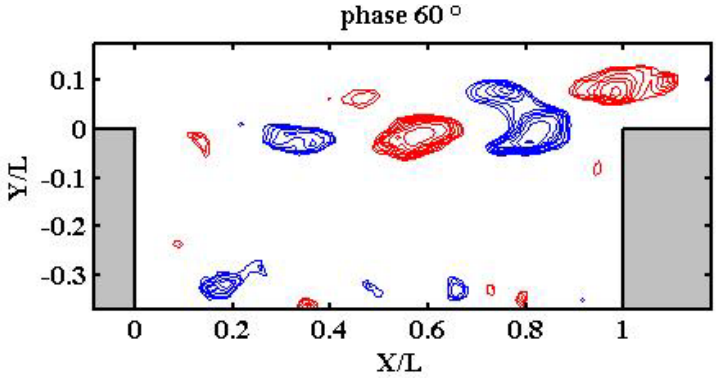

Fig 4-3: Example of phase-locked ensemble average: the PIV snapshots of the eddies shed by the upstream lip of a cavity under a grazing flow are synchronised with a wall pressure signal. Vorticity iso-contours are shown

An unusual example of such a phase-locked ensemble average is shown on Fig 4-3 and Fig 4-4 (M.C. Jacob N. Grosjean & M. Michard, 2004, *unpublished data*) for a flow past a cavity where a pressure signal in the

cavity (on the downstream wall) is synchronised with PIV measurements. Vorticity iso-contours and vertical (upwash) velocity fluctuations are plotted on Fig. 4-3 and Fig. 4-4 respectively. The PIV snapshots are triggered at a fixed phase of the periodic pressure signal (60° and 120° respectively for Figs. 4-3 and 4-4). This information may be used to model the wall pressure fluctuations on the forward facing wall of the cavity as a function of the incoming shear layer disturbances. This could then be fed into an analogy.

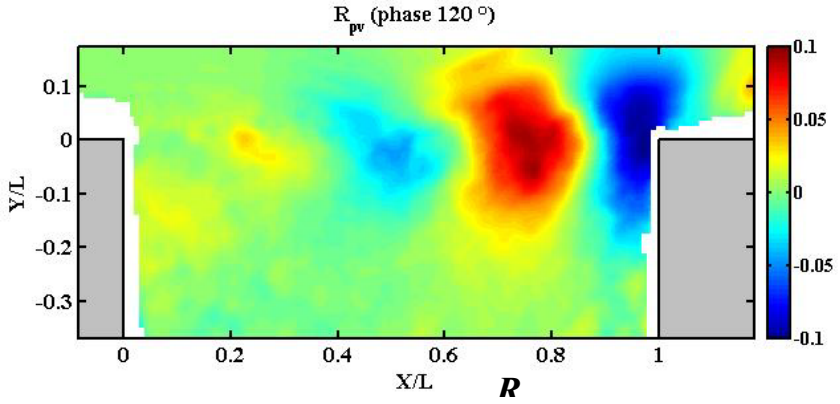

Fig 4-4 Flow past a cavity: two-point correlation between a pressure signal in the cavity and the upwash velocity obtained from PIV. The PIV snapshots are triggered by the phase of the periodic pressure signal.

Two-point space-time correlations:

Two-point space-time correlations are essential for flow self noise, as they evaluate the average time evolution of Reynolds stress components depending on their typical size. An illustration is shown on Fig 4-5 for the same cavity flow as on Fig 4-3 and Fig 4-4. Note that these measurements were carried out in 2004 when time-resolved PIV was not yet available: the time correlations were obtained by synchronising two PIV systems (two sources and two cameras).

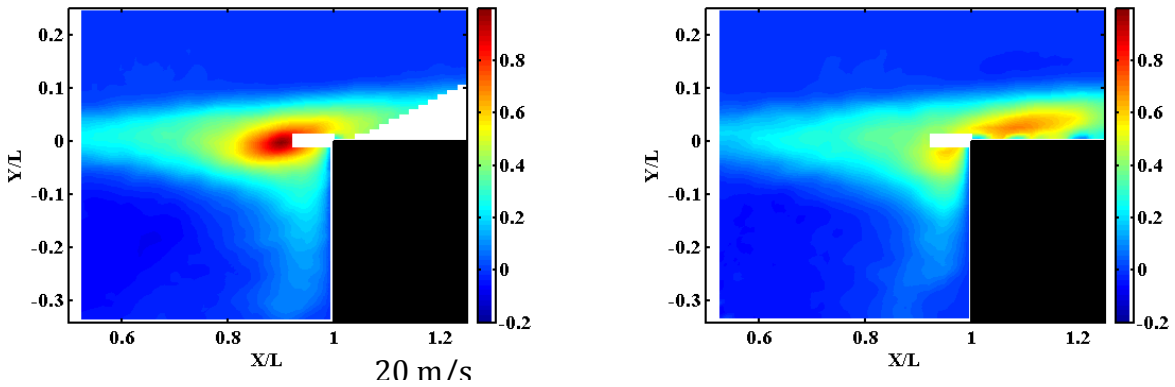

Fig 4-5 Space-time correlations of the streamwise velocity fluctuations $R_{uu}(\vec{x}, t; \vec{y}, t+\tau)$ for two correlation times: $\tau = 0$ (left) and $\tau = 500\ \mu s$ (right). The point $\vec{x}$ is located in the middle of the dark red spot of the left plot. In white zones, the PIV measurements are erroneous.

Many other measurement strategies or data processing techniques can be imagined to provide relevant information for specific problems, such as conditional averages for intermittent phenomena, vortex trajectory oscillations or separation bubble oscillations etc. Some of these will be illustrated on an application case in lecture n°11.

4.2 Noise induced by Aerodynamic probes

Aerodynamic probes may induce some perturbations due to the physical place they occupy in the flow: this is typically the case of HWA probes: they not only perturb the flow locally but may also pollute the sound signal. If a HWA probe is supported by a long rod, a broad peak about the corresponding shedding frequency (St ~ 0.2) may alter the sound field.

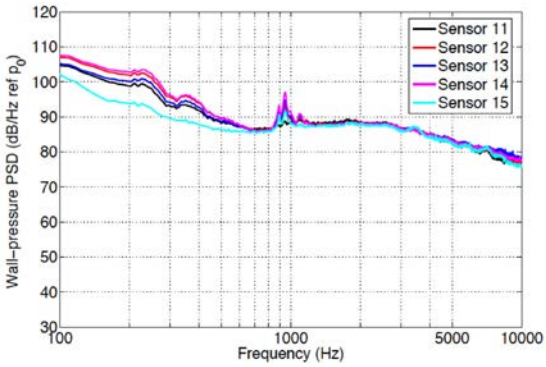

Fig 4-6 Disturbances on wall pressure spectra due to nearby located Hot Wire support: Strouhal peak about 920 Hz

To illustrate this, Fig 4-6 shows wall pressure spectra that were measured in the presence of a hot wire probe: in this case, the supporting rod had to be very long and thick because the probes reached the measurement from outside the flow through the shear layers at M~ 0.2. Therefore, the induced sound was loud enough to peak out of the wall pressure spectra along the NACA5510 mid-span trailing-edge.

Of course, Pitot probes that are used to determine the flow velocity have to be removed prior to any sound measurement.

Similarly wall pressure probes that are embedded in a fairing might perturb the flow: as a result the local flow field (velocity and pressure) may be flawed but the effect onto the far field is not expected to be significant. However, in many applications, microphones can be flush mounted into the wall and remotely connected to a wall pressure tap (as will be discussed in lecture n°3).

Optical measurement techniques

Optical techniques such as LDV and PIV are known to be less intrusive as Hot Wire Anemometry as far as the flow is concerned but their accompanying apparatus (laser source, cooling device, camera, carriage...) might act as strong reflectors in the anechoic room in some cases.

4.3 In-flow acoustic measurements – Examples

To conclude this section on measurements, we will show a few examples of in-flow acoustic measurements, as the topic will be detailed in lecture n°3.

4.3.1 HWA

Hot-wire probes measure all the fluctuations they experience, even acoustic velocity fluctuations. Usually, velocity fluctuations from sound waves are orders of magnitude smaller than aerodynamic ones. However, there are certain situations were they can be measured. One type of situation is when there are intense sound waves in the flow: tones from a turbofan engine, shockwaves; another type of situation corresponds to sound waves propagating in a very quiet flow.

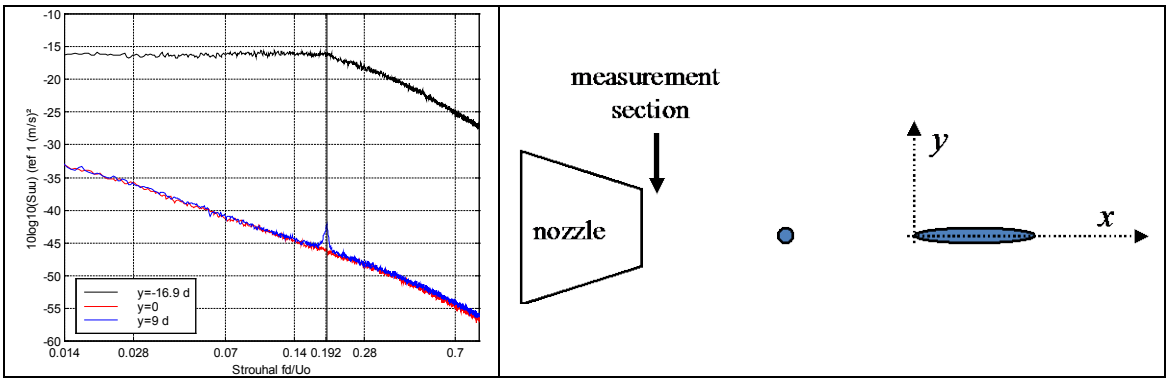

Fig 4-7 Hot Wire spectra showing the tonal sound radiation by the rod-airfoil tandem peaking out of the turbulence background (left). Sketch showing the measurement section (Right). d (cylinder diameter) = 0.01 m; M~0.2 – Re_d~ 48000, $Length/d = 30$; $Chord/d = 10$

An illustration of the latter is shown on Fig 4-7: the data was obtained near the nozzle outlet of the rod-airfoil experiment [15] mentioned in section 3.1.1. The turbulence level is about 0.8 % and the rod and airfoil emit in a frequency range where the turbulence spectrum is already 12-13 dB below its maximum. The streamwise velocity spectrum is plotted on Fig 4-7 on the flow central axis (obs. angle 180° "$y = 0$") away from the axis ("$y = 9\ d$") and in the aft port shear layer ("$y = 16.9\ d$"). Away from the axis in the quiet flow region a peak appears at the shedding frequency St-0.192. This peak is not present on the central axis of the flow since the rod radiation is dipolar and the airfoil cardioid radiation is also silent in that direction. In the shear layer, the flow turbulence is so intense that the sound peak cannot be seen. Note that the example discussed on Fig 4-6 is intermediate: the sound pressure density generated by the Pitot probe is above the non-negligible local boundary layer wall pressure fluctuations.

4.3.2 Wall pressure

Wall pressure measurements can also measure sound waves: one method is to measure the phase between two probes as illustrated on Fig 4-2. If the phase velocity is higher than or equal to the speed of sound, then the fluctuation may be that of a wave. Another way is to measure the wall pressure with a whole array of wall mounted pressure probes and to compute the wavenumber–frequency spectrum for modelling purposes [25]; the acoustic contribution may be observed for a particular value of the wave number ($k_0 = \omega/c_0$). Wall pressure fluctuations are further discussed in M. Roger's lecture n°3.

4.3.3 Schlieren technique

The Schlieren technique is often used to visualise shocks and turbulence in supersonic flows. The density gradients due slight pressure and temperature variations typically occurring in compressible flows are measured by the relative deviation of light rays crossing them. Successive density variations encountered along each ray path are summed up providing an integral of the density gradient in the direction of the light. Thus the technique is essentially qualitative. On Fig 4-8 the Schlieren technique is applied to visualise the axial density gradient of an under-expanded supersonic jet. The picture is taken from a movie: by comparing successive images, the movie also allows to visualise very slight density gradient variations that cannot be seen on a single picture.

The diamond shaped shock cell patterns are clearly shown as they increasingly interact with the turbulent structures from the shear layer. The ripples near the left upper corner are due to air entrained by the jet: on the associated movie they can indeed be seen moving slowly towards the jet and being entrained by the flow. On the movie (not on the picture), sound waves can be identified travelling into the upstream direction probably due to shock-associated noise but also in the downstream direction due to large scale Mach wave radiation.

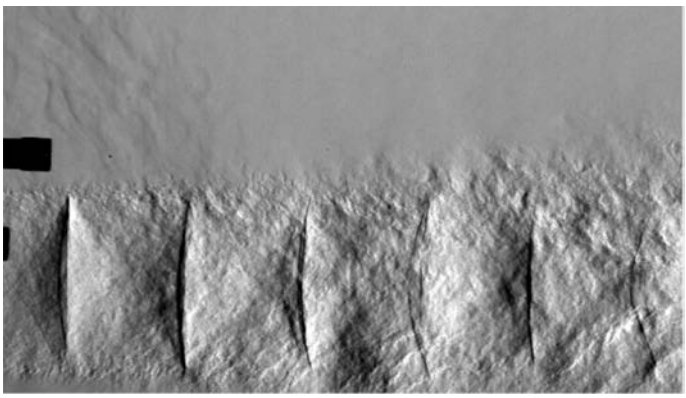

Fig 4-8 Schlieren picture of a supersonic jet (from a movie by Bertrand Mercier, ECL)

4.3.4 Causality techniques

As discussed in section 4.1.2, causality techniques can be used to estimate either the size or duration over which a turbulent structure is coherent, that is, its size or life-time in a statistical sense. Since sound waves are fully coherent over large distances regardless of their amplitude or their time dependence, they can be detected in a flow with appropriate causality techniques. For instance, subtracting the diagonal of a cross-spectral matrix obtained from a modal detection array in a duct is a simple way to partly separate local turbulence induced fluctuations from non-local sound fluctuations. More generally, when correlating sensors that are distant from each other, and making sure that they cannot be hit by the same convected turbulent structures (as might be the case for instance, if one is located downstream of the other), the observed correlations are very likely to be linked to sound waves. As mentioned in section 4.1.2, information about the phase shift between the probes and the resulting phase velocity, might provide additional clues when available.

Causality techniques may also be used to link a far field noise component with a particular flow mechanism, by correlating a flow-imbedded measurement to the far field. The Coherent Output Power (COP) spectrum method [26] and the 3 sensor method [27] are good candidates for this type of measurements. The main difficulty of these methods is to find signals in the source region that are sufficiently representative of the source mechanism, which implies that these signals are not blurred by spurious noise. The 3 sensor method is a first step to clean the in-flow measurements with respect of pseudo sound and other spurious fluctuations that may be felt independently by each probe. These concepts were validated in a transparent wind tunnel [28] and then applied to sources on high-speed trains [29] with appropriate in-flow probes. The COP technique will be explained in more detail in lecture n°3.

Techniques based on conditional averages may also be applied between the flow field and the far field, as will be shown and explained in lecture n°11.

CONCLUSION

After this quick overview of experimental aeroacoustics, the following lectures of the present series will specify more details about of the concepts introduced here and describe more applications.

REFERENCES

[1] V. Strouhal, Über eine besondere Art der Tonerregung, *Annalen Phys. Chem.* (Leipzig) **3(5)**, 216–251, (1878).

[2] J.W.S. Rayleigh, Aeolian tones, *Phil. Mag.,* **29**, 434–444, (1915).

[3] H.S. Ribner, The generation of sound by turbulent jets. *Adv. Appl. Mech*. **III**, Academic Press, (1964).

[4] M.J. Lighthill, On sound generated aerodynamically: 1. General theory, *Proc. Roy. Soc.,* **A 211**, 564–578, (1952).

[5] M.J. Lighthill, On sound generated aerodynamically. II. Turbulence as a source of sound, *Proc. Roy. Soc.,* **A. 222**, 1–32, (1954).

[6] K.S. Brentner, Direct numerical calculation of acoustics: solution evaluation though energy analysis, *J. Fluid Mech*., **254**, 267 -281, (1993).

[7] S.K. Lele, P. Moin, T. Colonius, B. Mitchel, *Direct computation of aerodynamic noise*, in Computational Aeroacoustics, Springer New York, 325-224, (1993).

[8] A. Witkowska, D. Juvé, J.G. Brasseur, Numerical study of noise from isotropic turbulence, *J. Comp. Acous.,* **5(3)**, 317-336, (1997).

[9] C. Bailly, W. Béchara, P. Lafon, S. Candel, Jet noise predictions using a $k-\epsilon$ turbulence model, *AIAA Paper n°* **93-4412**, (1993).

[10] N. Curle, The influence of solid boundaries upon aerodynamic sound, *Proc. Roy. Soc.,* **A 231**, 505–514, (1955).

[11] J.E. Ffowcs Williams, D.L. Hawkings, Sound generated by turbulence and surfaces in arbitrary motion *Phil. Trans. Roy. Soc.*, **A 264**, 321–342 (1969).

[12] B.T. Chu & L.S.G. Kovásznay, Interactions in a viscous heat-conducting compressible gas, *J. Fluid Mech.*, **3(5)**, 494–514, (1958).

[13] P. Laffay, M.C. Jacob, S. Moreau, J. Regnard, Experimental investigation of the transient bleed valve Noise, *AIAA Paper n°* **2017-3528**, (2017).

[14] C. Tam, M. Golebiowski, J. Seiner. On the two components of turbulent mixing noise from supersonic jets, *AIAA Paper* **n°96-1716**, (1996).

[15] M.C. Jacob, J. Boudet, D. Casalino, M. Michard, A rod-airfoil experiment as benchmark for broadband noise modelling, *J. Theoret. Comput. Fluid Dyn*., **19(3)**, 171-196, (2005).

[16] M. Gruber, *Airfoil noise reduction by edge treatments*, PhD thesis, Univ. Southampton (2012).

[17] M.C. Jacob, A. Louisot, D. Juvé, S. Guerrand, Experimental Study of Sound Generated by Backward-Facing Steps Under Wall Jet, *AIAA J.*, **39(7)**, 1254–1250, (2001).

[18] M. Roger, *Fundamentals of Aeroacoustics – Part I,* Lecture Notes – Ecole Centrale de Lyon, (2010).

[19] S. Moreau, M. Roger, Back-scattering correction and further extensions of Amiet's trailing-edge noise

model. Part II: Application, *J. Sound Vib.*, **323**, 397-425, (2009).

[20] E. Rademaker, P. Sijtsma, B. Tester, Mode detection with an optimised array in a model turbofan engine intake at varying shaft speeds, *AIAA paper n°* **2001-2181**, also *NLR TP*-**2002-132**, (2002).

[21] A. Finez, Etude expérimentale du bruit de bord de fuite à large bande d'une grille d'aubes linéaire et de sa réduction par dispositifs passifs, *Thèse de doctorat de l'Ecole Centrale de Lyon*, (2012).

[22] Blake, W. K., *Mechanics of Flow Induced Sound and Vibrations*. Academic Press, (1986).

[23] M.C. Jacob, E. Jondeau, B. Li, Y. Liu, Time resolved measurements of a tip leakage flow *Int. J. Aeroacoustics*, **15 (6-7)**, 662-685, (2016).

[24] M. Roger, J. Grilliat, Y. Rozenberg, J. Boudet, M.C. Jacob, Final report on improved self noise source models, *Deliverable D2.11, EU project PROBAND n°***AST4-CT-2005-012222**, (2006)

[25] G. Corcos, Resolution of pressure in turbulence, *J. acoust. Soc Am.*, **35**, 192-199, (1963).

[26] J. S. Bendat and A. G. Piersol, *Engineering Applications of Correlations and Spectral Analysis*. New York: John Wiley & Sons, Inc. (1993).

[27] J. Y. Chung, Rejection of flow noise using a coherence function method. *J. Acous. Soc. Am.*, **62**, 388-395, (1977).

[28] M.C. Jacob, G. Robert, N. Fremion, S. Guerrand, In-flow acoustic measurements on high speed trains, *AIAA paper n°* **2000-2011**, (2000).

[29] N. Frémion, N. Vincent, M. Jacob, G. Robert, A. Louisot, Aerodynamic noise radiated by the intercoach spacing and the bogie of a high-speed train, *J. Sound Vib.*, **231(3),** 577-593, (2000).